The Journal of Chemical Physics ARTICLE scitation.org/journal/jcp

Propagating molecular rotational coherences through single-frequency pulses in the strong field regime

Cite as: J. Chem. Phys. 151, 084312 (2019); doi: 10.1063/1.5099049
Submitted: 5 April 2019 • Accepted: 8 August 2019 •
Published Online: 30 August 2019

A. O. Hernandez-Castillo,[1,a] Chamara Abeysekera,[1,b] F. Robicheaux,[2,c] and Timothy S. Zwier[1,c]

AFFILIATIONS

[1] Department of Chemistry, Purdue University, West Lafayette, Indiana 47907-2084, USA
[2] Department of Physics and Astronomy, Purdue University, West Lafayette, Indiana 47907-2084, USA

[a] **Present address:** Department of Molecular Physics, Fritz-Haber-Institut der Max-Planck-Gesellschaft, Faradayweg 4-6, D-14195 Berlin, Germany.
[b] **Present address:** Intel Corporation, Hillsboro, Oregon 97124, USA.
[c] **Authors to whom correspondence should be addressed:** robichf@purdue.edu and zwier@purdue.edu

ABSTRACT

In the weak-field limit in which microwave spectroscopy is typically carried out, an application of a single-frequency pulse that is resonant with a molecular transition will create a coherence between the pair of states involved in the rotational transition, producing a free-induction decay (FID) that, after Fourier transform, produces a molecular signal at that same resonance frequency. With the advent of chirped-pulse Fourier transform microwave methods, the high-powered amplifiers needed to produce broadband microwave spectra also open up other experiments that probe the molecular response in the high-field regime. This paper describes a series of experiments involving resonant frequency pulses interrogating jet-cooled molecules under conditions of sufficient power to Rabi oscillate the two-state system through many Rabi cycles. The Fourier-transformed FID shows coherent signal not only at the applied resonant frequency but also at a series of transitions initially connected to the original one by sharing an upper or lower level with it. As the duration of the single-frequency excitation is increased from 250 to 1500 ns, the number of observed off-resonant, but dipole-allowed, molecular coherences grow. The phenomenon is quite general, having been demonstrated in Z-phenylvinylnitrile, E-phenylvinylnitrile (E-PVN), benzonitrile, guaiacol, and 4-pentynenitrile. In E-PVN, the highest power/longest pulse duration, coherent signal is also present at energetically nearby but not directly connected transitions. Even in molecular samples containing more than one independent species, only transitions due to the single species responsible for the original resonant transition are present. We develop a time-dependent model of the molecular/photon system and use it in conjunction with the experiment to test possible sources of the phenomenon.

I. INTRODUCTION

The majority of spectroscopic studies employing Fourier transform microwave techniques are based on the interaction of molecular two-level systems with a microwave radiation field. The theoretical description is based on the density matrix formalism, which models the sample of rotating molecules as an ensemble of two-level systems.[1] The evolution in time of a gaseous molecular ensemble is usually treated considering a homogeneous z-polarized field, and its description is based on the optical Bloch equations. These equations describe the time-evolution of the diagonal and off-diagonal density matrix elements corresponding to the populations N_a and N_b of the two levels $|a\rangle$ and $|b\rangle$ and their two-level coherence.[2,3]

When electromagnetic radiation interacts with a molecule through a two-level electric dipole interaction, a macroscopic polarization is produced which has a relaxation time of T_2, and a nonthermal equilibrium population distribution is produced which decays with a relaxation time of T_1.[4,5] Transient experiments

normally involve observing the effects of bringing an ensemble of two-level quantum-mechanical systems into or out of resonance with the radiation field on time scales short relative to the relaxation processes in the two-level system.[6] All transient phenomena involve the interplay of the polarization and population differences through their coupling with the electric field. Transient experiments on rotational states are classified as those involving coherent absorption and coherent spontaneous emission. Transient nutation is used to describe transient absorption, and free induction decay (FID) is used to describe spontaneous coherent transient emission.[7]

Chirped-pulse Fourier transform microwave (CP-FTMW) spectroscopy, first implemented in the Pate laboratory,[8] has since become widely used by the spectroscopy community as has been recently reviewed by Park and Field.[9] An important advance of CP-FTMW spectroscopy compared to Fabry-Perot cavity Fourier transform microwave spectroscopy[10] is that it is possible to perform a broadband excitation on a time scale shorter than the transient emission time. In a standard CP-FTMW experiment, after the transient absorption, the polarization of the molecular ensemble is observed in the absence of external electromagnetic fields (in the absence of the polarization pulse). Thus, the molecular coherence causes transient emission that propagates in the same direction as the electromagnetic pulse driving the transient absorption.[1]

Excitation that occurs under fast passage conditions in which the microwave frequency is swept over the absorption profile produces transient absorption during the sweep followed by transient emission after the sweep.[11,12] Depending on the experimental conditions, a large change in population difference of the states in resonance or the coherence of the two-level ensemble can be achieved. Therefore, the coupling of the molecules to the electric field is particularly important, and it is characterized by the Rabi frequency of the population oscillating between the two states of the resonance. When a frequency chirp is applied under conditions of strong coupling with the electric field, the process is known as rapid adiabatic passage (RAP) or adiabatic rapid passage (ARP) and is a well-known technique to selectively prepare atoms and molecules in specific states using, for example, chirped lasers.[13,14] In the microwave region, population inversion can be achieved through chirped excitation of rotational resonances.[12,15]

Since its invention, the method of CP-FTMW spectroscopy has been used to study a wide range of molecules, free radicals,[16,17] and molecular clusters and to probe chemical kinetics and reaction dynamics.[18,19] The versatility of the method is also being put to use in double-resonance experiments[20–23] and in coherent techniques based on the application of frequency-agile pulse sequences.[24,25] Following the work of Neill *et al.*,[22] we have recently described an experimental method that selectively modulates the intensities of a set of transitions due to a single component in a gas phase mixture.[26] The algorithm originally devised to produce the set of transitions involved first probing the sample with one or more single-frequency microwave pulses in the strong field regime, where a phenomenon not previously described in the literature was observed.

Even though the molecular response to microwave pulses in the strong field regime has not been previously explored in a systematic way, there are simpler systems where interaction of quantum systems with a strong oscillating electric field has been modeled.[27] For example, in atomic cavity quantum electrodynamics (QED), an isolated atom interacts with an electric field, giving rise to coherent oscillations of a single excitation between the atom and the cavity at the vacuum Rabi frequency, which can be observed when the Rabi frequency exceeds the rates of relaxation and decoherence of both the atom and the field.[28] Furthermore, the interaction of a strong *E*-field and the quantum system is also important in the time domain signals created in Rydberg atoms in three-dimensional microwave cavities[25,29,30] or in alkali atoms exposed to radiation in very small optical cavities where the spacing between vacuum levels is large.[31]

The present work focuses on the experimental and theoretical discoveries associated with an application of (nearly) monochromatic microwave pulses resonant with molecular rotational transitions, operating in the strong field regime. A set of experiments that helped characterize the observed phenomena are described, including the effect that collisions, pulse length, and amplitude of the microwave field have on the off-resonant coherence signals. Finally, the different attempts to model the phenomena are described.

II. EXPERIMENTAL METHODS

For much of the current work, a commercial mixture of (E)- and (Z)-phenylvinylnitrile (PVN) (97%, Alfa Aesar) was used as a molecular sample, providing a model system with two isomers, a large dipole moment and good signal-to-noise ratio for testing the phenomena. The liquid sample was absorbed on cotton and placed into a stainless-steel sample holder that was located immediately behind the pulsed valve. The sample was heated to ~80 °C to obtain sufficient vapor pressure and entrained in a supersonic expansion. To test the generality of the phenomenon, similar experiments were carried out on a series of other molecules. For benzonitrile, a commercial sample (98%, Sigma-Aldrich) was used at its room temperature vapor pressure. 4-pentynenitrile (97%, Sigma-Aldrich) and guaiacol (98%, Sigma-Aldrich) were heated to 120 °C and 110 °C, respectively.

The experiments were performed in a vacuum chamber originally designed by Dian and co-workers.[32] The molecules were cooled in a pulsed supersonic expansion (General Valve Series 9, 1 mm orifice diameter, 500 μs duration, 10 Hz) by entraining them in helium with a backing pressure of 2.3 bars unless indicated otherwise. The chamber's base pressure is 1×10^{-6} mbar with an operating pressure of ~3×10^{-5} mbar. The distance from the nozzle orifice to the centerline of the orthogonal microwave horns is ~12 cm. As described in more detail in the supplementary material, using the measured rotational temperature of $T_{rot} \sim 1$ K, we estimate that a PVN molecule experiences a hard-sphere collision with a He atom approximately every 25 μs.

The electronics have been described elsewhere,[17,26] so here we only provide a brief overview of the experimental setup. The chirps are generated by a 10 GS/s arbitrary waveform generator (AWG; Tektronix 7101), which is referenced by a 100 MHz quartz oscillator which is driven by a 10 MHz-Rb-disciplined crystal oscillator (Stanford Research Systems FS725). The waveform is multiplied with a quadrupler (Phase One PS06-0161). After multiplication, a 200 W traveling wave tube amplifier (TWTA; Amplifier Research model

AT4004) is used to amplify the single frequency pulses (SFPs). The output is broadcasted into the vacuum chamber through a broadcasting horn (Amplifier Research model AT4004, 8–18 GHz) and polarized the sample molecules, which then undergo a free induction decay (FID). The time domain signal (FID) is collected with a second broadcasting horn and amplified by a +45 dB low noise amplifier (MITEQ AMF-6F-0600-1800-15-10P). The FID collection is initiated ~160 ns after the high power chirp, which incorporates the switching speed of the SPST-switch. The amplified signal is down-converted and phase coherently averaged by a 13 GHz, 40 GS/s real time digitizer (Guzik ADC6131); for these experiments, the FID duration was 16 μs. During a typical experiment, 25 FIDs are recorded per gas pulse with a spacing between excitations of 20 μs. The time domain spectrum is fast Fourier transform to obtain the frequency domain spectrum.

The fundamental experiment that is the subject of the present investigation is remarkably simple. After recording a broadband microwave spectrum of the sample of interest under weak-field conditions, a molecular rotational transition was chosen for resonant excitation. The arbitrary waveform generator was programmed to output a single-frequency sine wave, typically tuned to the peak frequency of a microwave transition with a substantial transition dipole moment (TDM). Generally, for a rectangular pulse, the turn on and turn off time was ~5 ns. The duration and power of the resonant pulse are under experimental control. Windowing functions were typically applied in order to change or control the wings and shape of the frequency signal applied, using rectangular, Tukey, or Gaussian window functions. In order to minimize edge effects, SFPs longer than 100 ns were typically used.[33]

III. THEORETICAL METHODS

We developed three generalized programs to model the time-dependent quantum mechanics of arbitrary microwave pulses interacting with the rotational states of a molecule.[34] All of the programs use the following Hamiltonian:

$$\hat{H} = \hat{H}_{rot} + \hat{H}_{field}, \tag{1}$$

where the solutions to $\hat{H}_{rot}$ are the rotational eigenstates of an asymmetric top, and

$$\hat{H}_{field} = -\hat{\mu}_z E_0 W(t) \cos(\omega_{MW} t), \tag{2}$$

where $\hat{\mu}_z$ is the electric dipole moment operator, E_0 is the amplitude of the microwave electric field, ω_{MW} is the microwave frequency, and $W(t)$ is the window function which is discussed in Sec. IV. $\hat{H}_{field}$ depends on the electric-field associated with a time-dependent microwave pulse, here modeled simply as a pure cosine wave polarized in the z-direction. In all of the programs, the eigenstates of the asymmetric top rotational Hamiltonian, $\hat{H}_{rot}$, are used as the basis to expand the full Hamiltonian. The Hamiltonian could also be expanded to include nuclear hyperfine and other terms that split the rotational levels, but these effects were not included in our calculations.

Two of the programs were based on two different methods of solving for the time evolution of the superposition of rotational states. The first method gives a more accurate treatment for the case that the microwaves have constant strength and frequency, but it cannot easily be used to model the turn-on and -off of the microwaves or any chirp. This method is, essentially, a Floquet treatment of the Hamiltonian.[35] This method is useful because the eigenstates and eigenvalues can be used to calculate $U(t, t_0)$ for any duration $t - t_0$.

The second method does not explicitly use $U(t, t_0)$ but instead directly solves for the time evolution of the wavefunction using the leapfrog algorithm

$$|\psi, t_0; t + \Delta t\rangle = |\psi, t_0; t - \Delta t\rangle - \left(\frac{2iH(t)\Delta t}{\hbar}\right)|\psi, t_0; t\rangle, \tag{3}$$

where Δt is the time step and the one step error is proportional to Δt^3. This method has the advantage of easily incorporating the window function and any chirp but has the disadvantage of needing more computational steps to handle longer propagation times. By using the full $H(t)$ in Eq. (3), we are going beyond the rotating wave approximation so that possible multiphoton and/or effects due to nonresonant transitions are included. The other difficulty is that the time step needs to be smaller as the energy spread and the basis is increased. In the actual calculation, the wave function was expanded in the basis of eigenstates of the asymmetric top rotational Hamiltonian ($|\varphi(t)\rangle = \sum_n |\varphi_n\rangle C_n(t)$). Convergence was checked with respect to the time step and the number of basis functions that compose the wave function. The basis functions were chosen by an energy condition: all asymmetric top states within an energy of $C \cdot \hbar \cdot \omega_{MW}$ of either of the resonance states were included and C was increased until the calculated FID stopped changing.

Finally, when the microwaves are off, there is an oscillating dipole $\mu(t)$ because the microwaves produce coherences between the rotational states. This oscillating dipole depends on the initial state before the microwaves are turned on, the coefficients of the asymmetric top eigenstates, the energy differences between these states, and the dipole matrix elements between the states ($\mu_{n'n} = \langle\varphi_{n'}|\hat{\mu}_z|\varphi_n\rangle$). We assume that the molecules start in an incoherent superposition of rotational eigenstates weighted by the Boltzmann factor at a rotational temperature 1.43 K. We did not try to select individual initial states but included all states contributing to the Boltzmann distribution. The total $\mu(t)$ results from the weighted sum over the possible initial states.

The third program solved the full density matrix, where an N × N matrix was propagated (N being the number of states), allowing the molecule to start in all of the states (up to M_J = J) with the appropriate Maxwell-Boltzmann weight. The time propagation for the Hamiltonian terms was carried out using the direct solution for the time dependent wave function [Eq. (3)]. Solving the density matrix equations allowed us to test various mechanisms, e.g., collisions and decoherence, that are hard to model using wave functions.

IV. RESULTS

When resonantly exciting a molecular rotational transition with a single frequency pulse under full power conditions on our traveling wave-tube amplifier (TWTA), we noticed early in our investigations that coherent signals were produced from a set of conformer specific transitions, not just from the transition resonantly excited. Figure 1 illustrates this behavior using PVN as a

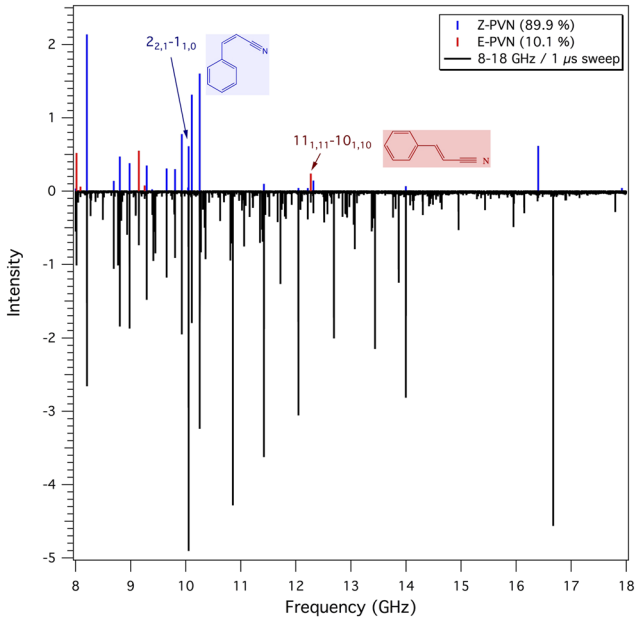

FIG. 1. Comparison between a broadband spectrum of PVN taken under linear fast passage conditions (10% TWTA gain, in black) with the results of two 1 μs single-frequency pulse experiments, with frequency fixed on the $2_{2,1}$-$1_{1,0}$ transition (10 052.50 MHz) of Z-PVN (in blue) and the $11_{1,11}$-$10_{1,10}$ transition (12 270.31 MHz) of E-PVN (in red). The sample contains 90% Z-PVN and 10% E-PVN. The vertical axis is in mV, enabling comparison of the signals generated in SFP vs broadband conditions. Each spectrum shown is the result of averaging the FIDs from 2.5×10^4 microwave pulses. The molecular parameters of both isomers are shown in Table S1.

test molecule, taking advantage of its large dipole moment to obtain strong signals with comparatively little signal averaging. Initially, it was expected that when sending a SFP, only the excitation frequency would show up in the resultant spectrum. However, when the frequency of the excitation pulse was fixed on the $2_{2,1}$-$1_{1,0}$ (10 052.500 MHz) transition of Z-PVN, an application of a 1 μs long pulse at 100% TWTA power (200 W) produces a Fourier-transformed signal that contained 13 transitions belonging to Z-PVN (shown in blue in Fig. 1), while no transitions associated with E-PVN appeared. Alternatively, when the same experiment was carried out with the single-frequency pulse (SFP) resonant a transition in E-PVN (the $11_{1,11}$-$10_{1,10}$ at 12 270.313 MHz), an analogous 1 μs pulse at 100% TWTA power produces a set of five isomer specific transitions shown in red.

Even though the transition dipole moment of the Z-PVN transition used for the SFP experiment in Fig. 1 is smaller than that used for E-PVN, the number of transitions appearing above the noise level in Z-PVN is almost three times greater than in E-PVN. The appearance of this large number of off-resonant transitions in the molecular FID called for further exploration, especially since the signals are isomer-specific, and hence not likely to be due to some artifact, at least not in its entirety. In what follows, we describe a series of tests designed to uncover the physical mechanism that generates these nonresonant transitions.

A. Windowing functions

The spectra obtained in Fig. 1 used "rectangular" pulses in that the input to the arbitrary waveform generator (AWG) involved an application of a single frequency pulse of constant amplitude over a fixed time duration. Such pulses have wings in frequency space, which could lead to poor spectral isolation and the possibility that the low-intensity spectral wings to the pulse could provide the frequencies needed to excite other molecular transitions. Notably, this simple explanation would not account for the species specificity demonstrated in Fig. 1. Nevertheless, it was important to test if by using cleaner pulses, the phenomenon was still present. To do so, we initially applied a Gaussian window function to the SFP. When using this window function, a decrease in intensity was observed in the overall spectrum; nonetheless, the number and pattern of off-resonant transitions appearing in the strong-field SFP experiment remained the same. Once the single frequency pulse was too narrow in time, the resulting spectrum slowly shifted toward that expected for a SFP in the weak field regime, with transition intensity present in fewer transitions with less intensity, until only the resonant transition appears in the spectrum, consistent with the decreasing total energy delivered to the sample. Then, upon shortening the pulse duration still further, the resonant spectral energy delivered would continue to decrease as its shorter duration broadens the pulse in the frequency domain. A Kaiser window[36] was also used on the single frequency pulses, and no change was observed in the number or intensity of the off-resonant transitions.

Finally, a tapered cosine or Tukey window[37] was applied as a third test of its effects on the SFP signals. One advantage of the Tukey window, which we experimentally observed, is that the amplitude of the transient signals in the time domain is less likely to be altered. The Tukey window, w(n) is defined by the following equation:

$$w(n) = \begin{cases} \frac{1}{2\left\{1+\cos\left(\frac{2\pi}{r}\left[n-\frac{r}{2}\right]\right)\right\}}, & 0 \le n < \frac{r}{2}, \\ 1, & \frac{r}{2} \le n < 1-\frac{r}{2}, \\ \frac{1}{2\left\{1+\cos\left(\frac{2\pi}{r}\left[n-1+\frac{r}{2}\right]\right)\right\}}, & 1-\frac{r}{2} \le n \le 1, \end{cases} \quad (4)$$

where r is the ratio of the length of the cosine-tapered section to the entire window length and n is a point in a linearly spaced vector. In the limit that $r = 0$, one has a rectangular window, while at $r = 1$, a Hann window is being applied.[38]

A series of scans were carried out in which the SFP signal was collected for excitation pulses in which r was increased from 0.25 to 0.75 in increments of 0.1. Again, there was no noticeable change in the number or pattern of the off-resonant transitions with change in r. We conclude on the basis of these tests that any frequency broadening present when using a rectangular single-frequency pulse was not the reason for the appearance of the off-resonant transitions when pumping a transition with a single frequency pulse.

The tests with different window functions also showed clearly that, as the length of the SFP is shortened and therefore the off-resonant frequency components broadened, adding a window function counteracted this effect and made the resonant frequency more selective. Moreover, adding a Tukey window reduced the leakage just as effectively as a Kaiser or Gaussian window, without a big loss

in signal size. Therefore, for the rest of the experiments presented in succeeding sections, a Tukey window was used.

In the time dependent calculations that used windowing functions, we found that the widths of the FID lines were determined by the duration of the turn on/off of the microwaves and not the Rabi frequency when the number of Rabi oscillations was greater than ~5.

B. Off-resonant output from the TWTA

As a high-powered microwave component, the TWTA is potentially also a source of distortion of the AWG input (principally through amplification of harmonics) or of adding noise components to it. In order to make sure that the observed phenomenon was not due to electronic noise or power noise from the TWTA, the intensities of the nonresonant transitions were measured as a function of detuning from resonance. Figure 2 shows the effect of detuning the excitation frequency from resonance for a Z-PVN ($6_{1,6}$-$5_{0,5}$, 9928.90 MHz) *b*-type transition. For these tests, a 1 μs SFP was used, with the TWTA set to full power.

A similar series was carried out on the $8_{1,7}$-$7_{1,6}$ transition (9448.75 MHz) of E-PVN (Fig. S2). In E-PVN, all resonant and nonresonant molecular signals were lost when the pulse was 15 MHz off-resonance, whereas for Z-PVN, detuning of only 10 MHz off-resonance was sufficient. This is consistent with the larger dipole moment present in E-PVN relative to Z-PVN. We conclude on this basis that resonant excitation of a molecular transition is essential for observation of the nonresonant signal from other molecular transitions and that the drop-off in nonresonant signal depends sensitively on the inherent transition strength of the resonant and nonresonant transitions.

C. Pulse power and duration

The SFP only creates coherences in off-resonant transitions when the oscillating electric field is strong and can couple with a nonzero transition dipole moment for the off-resonant transition. In order to understand the physical basis of the observed phenomena, it is important to assess experimentally the number and quantum state make-up of the transitions that appear in the SFP spectrum as a function of TWTA power (or more precisely, electric field strength) and pulse length, both of which are related to strength with which the molecular transition is driven by the resonant microwave field.

While the molecular rotational states comprise a manifold that is much more complicated than an idealized two-level system, it is still instructive to begin our discussion with a simple two-state system coupled by an oscillatory driving field. When that driving field is resonant with the transition between these two states, they cyclically absorb and re-emit photons in a Rabi cycle. The frequency of fluctuations in the populations between the two levels involved in

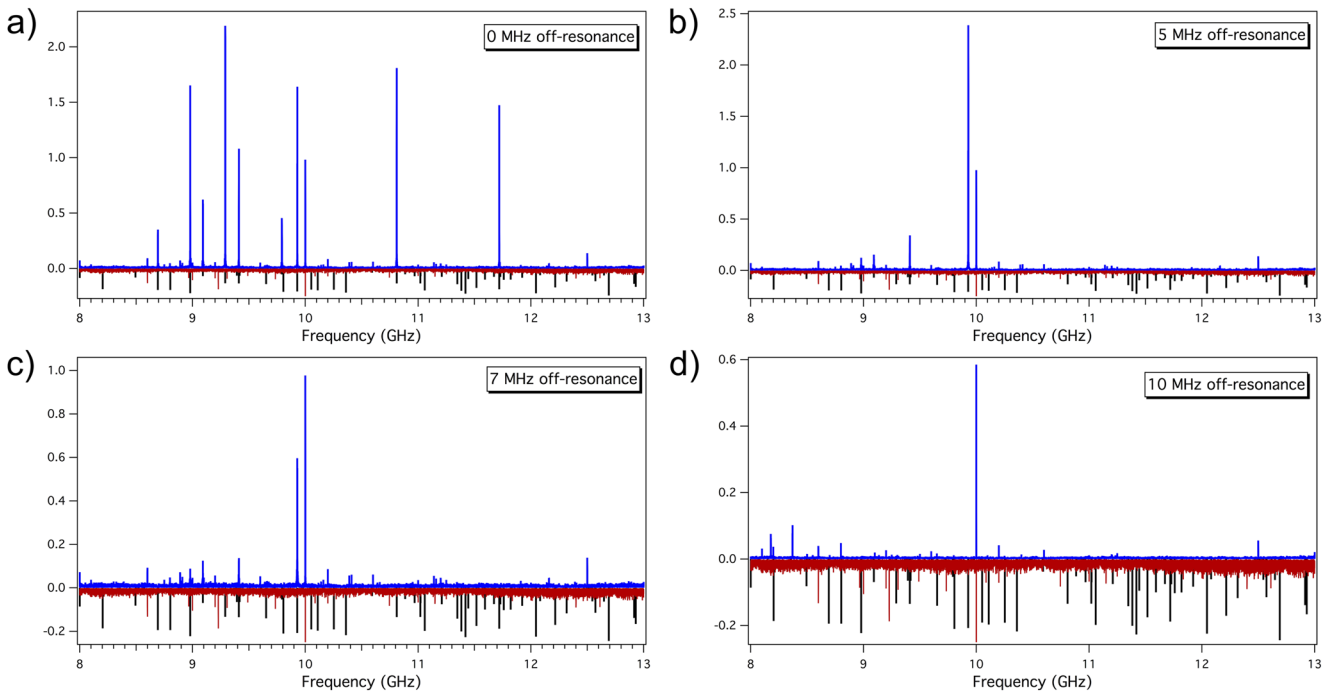

FIG. 2. Comparison of SFP spectra of Z-PVN generated by a series of single-frequency pulses recorded as a function of detuning from the $6_{1,6}$-$5_{0,5}$ resonance at 9928.875 MHz by (a) 0, (b) 5, (c) 7, and (d) 10 MHz, respectively. The spectra with molecular signal present are shown in blue. Background scans obtained by sending the respective single-frequency-pulse without any molecular sample present are shown in red, identifying spurious lines. The simulated broadband spectrum for Z-PVN using the experimentally determined rotational constants is shown for reference in black. Note the change in vertical scale with detuning. Vertical axes are in mV, while the noise threshold is 0.01 mV.

the process is called the Rabi frequency and is proportional to the strength of the coupling of the molecular transition with the oscillating the electric field. If the radiation is at the resonant frequency of transition i, the Rabi frequency is defined as

$$\Omega_i = \frac{\mu_i E_0}{\hbar}, \quad (5)$$

where μ_i is the transition dipole moment for transition i and E_0 is the electric field amplitude.[39] A Matlab program that calculates the transition matrix element and Rabi frequency was developed, using the output of Pickett's SPCAT program[40] to calculate the reduced transition matrix element. What we surmise on this basis is that, if the molecular states involved in the transition could be treated as a 2-state system, for the transition dipole moments and electric fields estimated to be present in the region between the horns, the states would be driven through many Rabi cycles. In what follows, we use this simple calculation just as a way of tracking the strength of the interaction, recognizing that mechanisms such as the M_J dependence of the TDM and spatial inhomogeneities in the E-field could dephase the Rabi cycling. The Matlab program and these dephasing mechanisms, as well as the experimental data that show the rapid dephasing of the coherence amplitude, are discussed further in the supplementary material.

Figure 3 presents two SFP spectra of Z-PVN recorded at 10% and 100% of full microwave power, showing a clear correlation between the number of transitions appearing in the SFP spectrum and the magnitude of the microwave power. Note that the off-resonant signals are sizable, with typical signal-to-noise ratios in Fig. 3(b) of greater than 60 after averaging 100 000 FIDs. More specifically, as Fig. 3(a) illustrates, with a 1 μs long SFP resonant with the $9_{0,9}$-$8_{0,8}$ (13 060.37 MHz) rotational transition in Z-PVN, only the resonant transition appears in the spectrum when 10% of the full power of the TWTA (~20 W, 3500 V/m) is used. However, at full TWTA power (100%, 200 W, 11 000 V/m), there are 11 transitions contributing to the spectrum [Fig. 3(b)]. Note that at the powers available with the TWTA, when this power is concentrated on a single resonant microwave transition, we estimate that, in a 2-level system, the transition would undergo 26 (10%) to 83 (100%) Rabi cycles during the 1 μs pulse. Electric field strengths of this magnitude are matched only in certain waveguide FTMW experiments; however, typical pulse lengths used in that case are almost 100 times shorter.[1] Therefore, the conditions used here are decidedly different conditions than is the norm under linear fast passage conditions.

To explore this general phenomenon further, a series of SFP experiments were conducted in which the TWTA power was increased systematically. These were performed when probing three different transitions for Z-PVN and two transitions for E-PVN. In each case, the same behavior was observed, in which the number of off-resonant transitions appearing in the SFP spectrum increased systematically as the power increased until a point at which only the intensity pattern changed, and then where (seemingly) steady-state conditions were reached in the intensities of the main transitions.

Since changing the pulse length also varies the total power experienced by the resonant two-level system, a series of experiments was

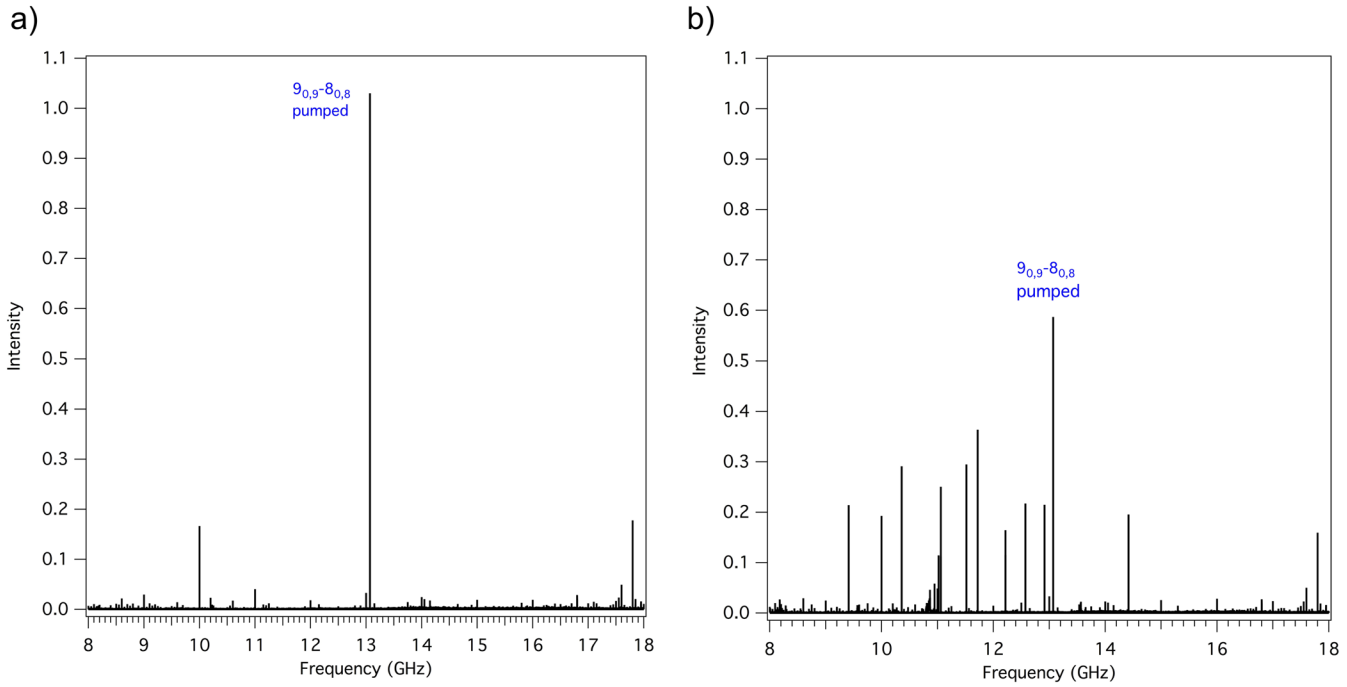

FIG. 3. Single frequency pulse (1 μs duration) resonant with the $9_{0,9}$-$8_{0,8}$ transition of Z-PVN, taken at (a) 10% TWTA gain (20 W, 3500 V/m) and (b) 100% TWTA gain (200 W, 11 000 V/m). The vertical scales are in mV with noise levels of 0.005 mV. See text for further discussion.

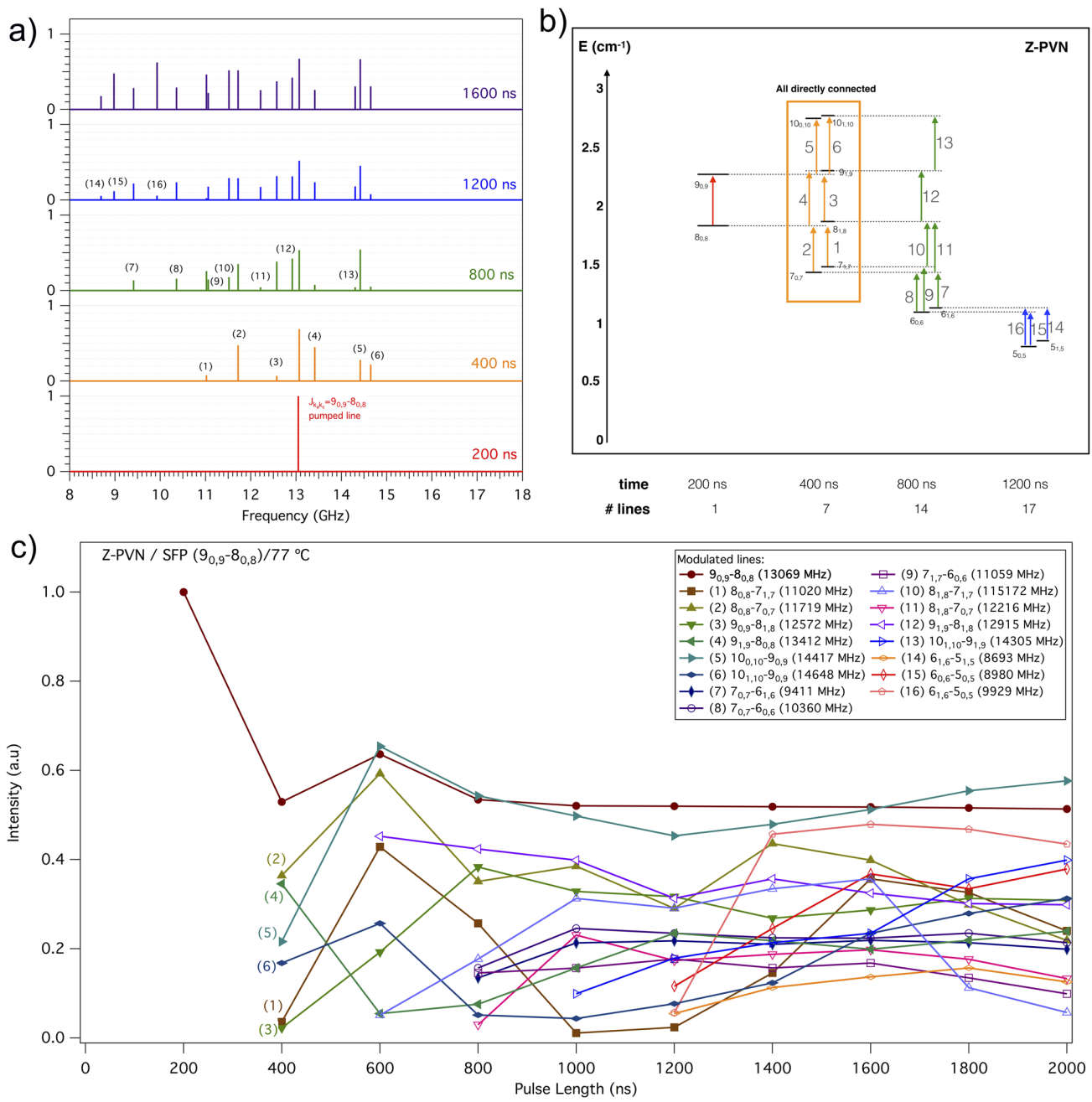

FIG. 4. (a) Comparison of single frequency pulse spectra taken as a function of the time duration of the single-frequency pulse resonant with $9_{0,9}$-$8_{0,8}$ transition of Z-PVN at 13 069.37 MHz. The labels match the numbered transitions in Table I. The vertical axis for all scans is normalized to the intensity of the resonant transition at 200 ns pulse duration. (b) Energy diagram for the resonant and off-resonant transitions that appear following SFP excitation with the indicated pulse duration. The colors in (a) and (b) match the different pulse lengths. (c) Plot of the intensities of the resonant and nonresonant transitions relative to the resonant transition at 200 ns pulse length, as a function of pulse duration (ns). While the intensity of the resonant transition under conditions of a $\pi/2$ pulse was not recorded for PVN, a corresponding study in benzonitrile showed that the off-resonant transitions were about 5–10 times smaller than the $\pi/2$ pulse intensity (Fig. S1).

carried out for both PVN isomers in which the length of the SFP was systematically increased at fixed TWTA power (in the strong field regime). In what follows, we show results for *a*-type transitions of both isomers of PVN. However, during the course of this study, similar behavior was observed for several transitions differing in type and initial rotational states.

Figure 4(a) shows a series of SFP spectra for Z-PVN with resonant "drive" frequency resonant with the $9_{0,9}$-$8_{0,8}$ transition at

13 069.37 MHz, for selected single-frequency pulse lengths from 200 to 1600 ns. In each case, a Tukey window with $r = 0.3$ was used when generating the pulses. With a pulse length of 200 ns, only the resonant transition appears in the spectrum as would be the expectation under low power conditions. However, by 400 ns pulse duration, six nonresonant transitions are clearly visible, and this number continues to grow systematically with pulse duration, reaching 16 new transitions at a pulse length of 1200 ns. The specific transitions that appear at each step are shown in the energy level diagram of Fig. 4(b). The reader should note that the spectra in Fig. 4(a) and all subsequent figures show only the intensities of the SFP transitions that are larger than the noise threshold of 0.01 mV and are not in the blank.

A plot of the intensities of the drive and 16 off-resonant transitions for the full data set is shown in Fig. 4(c). Note that between 1200 and 2000 ns pulse lengths, no new transitions of Z-PVN appear in the 8–18 GHz region. The intensity of the resonant transition reaches a steady state value about one-half its intensity at 200 ns pulse duration. Interestingly, the intensities of several of the directly connected transitions 1–6 show reproducible oscillations in intensity with increasing pulse duration. The intensity of the resonant and the directly connected transitions change little at long pulse durations.

Several important deductions can be drawn from these data. First, all of the new transitions appearing in the 400 ns SFP spectrum share a lower or upper energy level with the pumped transition and therefore are referred to as "directly connected" transitions. Second, all the observed nonresonant transitions are allowed transitions that appear with good strength in the broadband spectrum. Table I shows the list of transitions appearing in the SFP spectra of Fig. 4 and their calculated transition dipole moments (TDM) in Debye. In Z-PVN, these are either *a*-type or *b*-type transitions. Third, at every stage, the new transition(s) that appear share an energy level with either the pumped transition or an off-resonant transition previously induced. This means that transitions appearing following longer-pulse excitation sometimes share neither the upper or lower levels with the originally pumped transition; that is, they are not directly connected to the drive transition. Indeed, all transitions that appear after the first six [Fig. 4(b)] are in this category. Fourth, even though the transition dipole moments of the transitions between lower energy levels (smaller J_{KaKc}) are generally smaller, these transitions seem more likely to be present in the SFP spectrum than those between higher rotational energy levels.

The same set of experiments was carried out while resonantly exciting the $8_{0,8}$-$7_{0,7}$ (9148.89 MHz) transition of E-PVN (Fig. S3). The same qualitative behavior was observed with more off-resonant transitions appearing as the pulse duration increased. By comparing E-PVN and Z-PVN, one sees that, for the same pulse length, the number of off-resonant transitions in E-PVN is significantly less than in Z-PVN. Notably, in E-PVN, only *a*-type transitions appear as off-resonant transitions, mirroring the intensity patterns of one-photon transitions in the linear fast passage regime. Since the broadband spectrum of E-PVN is almost exclusively made up of a-type transitions (since $\mu_a = 8\ \mu_b$), but Z-PVN nearly equal intensity *a*- and *b*-type transitions, the E-PVN SFP spectra have many fewer transitions than in Z-PVN.

Notably, at longer pulse lengths, transitions appear in the E-PVN SFP spectra (Fig. S3) that do not share either a lower or upper level with the drive transition. Since *a*-type transitions follow a ΔK_a even selection rule, nonresonant transitions involving $K_a = 1$ levels cannot be produced by *a*-type transitions from $K_a = 0$. So, for instance, the $8_{1,8}$-$7_{1,7}$ off-resonant transition at 8935.415 MHz in the 1000 ns pulse length SFP spectrum of E-PVN is not connected either directly (by sharing a level with the drive transition) or indirectly (via a sequence of dipole-allowed nonresonant transitions) to the $8_{0,8}$ upper level or $7_{0,7}$ lower level of the resonant transition. This puzzling result requires coherence to be transferred between non-connected levels. Admittedly, weak *b*-type transitions are allowed even in E-PVN, but since $\mu_b \cong 0.63$ D, these *b*-type transitions have much smaller transition dipole moments, by about a factor of 50, than a corresponding *a*-type transition. A list of the transition dipole moments and frequencies of the modulated transitions in E-PVN is shown in Table S2.

D. Molecular properties

In order to test that these effects are a general response of polar molecules experiencing strong field excitation and to better understand how the off-resonant transitions depend on molecular properties, we carried out SFP experiments on three additional molecules: benzonitrile ($C_6H_5C{\equiv}N$), 4-pentynenitrile

TABLE I. Off-resonant transitions appearing in the FTMW spectrum following excitation with a single frequency pulse of varying duration that is resonant in frequency with the $9_{0,9}$-$8_{0,8}$ transition of Z-PVN. The calculated transition dipole moments (TDMs) associated with $m_J = 0$ in Debye are included. The transition numbering mirrors that in Fig. 4.

	Transition	TDM (D)	Frequency (GHz)		Transition	TDM (D)	Frequency (GHz)
1	$8_{0,8}$-$7_{1,7}$	1.4126	11 020.2500	9	$7_{1,7}$-$6_{0,6}$	1.4047	11 058.8750
2	$8_{0,8}$-$7_{0,7}$	1.6596	11 719.5625	10	$8_{1,8}$-$7_{1,7}$	−1.6547	11 517.1875
3	$9_{0,9}$-$8_{1,8}$	1.4474	12 572.2500	11	$8_{1,8}$-$7_{0,7}$	1.4322	12 216.1875
4	$9_{1,9}$-$8_{0,8}$	1.4576	13 412.1875	12	$9_{1,9}$-$8_{1,8}$	1.6564	12 915.2500
5	$10_{0,10}$-$9_{0,9}$	1.6590	14 417.4375	13	$10_{1,10}$-$9_{1,9}$	−1.6576	14 305.5000
6	$10_{1,10}$-$9_{0,9}$	1.4795	14 648.2500	14	$6_{1,6}$-$5_{1,5}$	−1.6478	8 692.9375
7	$7_{0,7}$-$6_{1,6}$	1.3678	9 411.0625	15	$6_{0,6}$-$5_{0,5}$	1.6638	8 979.6250
8	$7_{0,7}$-$6_{0,6}$	−1.661	10 360.0625	16	$6_{1,6}$-$5_{0,5}$	1.3786	9 928.8750

(HC≡C−$(CH_2)_2$−C≡N), and guaiacol (*o*-methoxy phenol). In each case, the same qualitative behavior is observed. Off-resonant transitions appeared when resonant, single-frequency pulses were applied at high powers where many Rabi oscillations occurred during the duration of the pulse.

Benzonitrile has C_{2v} symmetry and therefore a dipole moment exclusively along the *a*-axis. Figure 5(a) shows a series of SFP experiments, using the $4_{0,4}$-$3_{0,3}$ (10 855.25 MHz) transition as a resonant step, while increasing the length of the pulse (TWTA ~50%). The first transitions to appear (1000 ns SFP) are the $3_{0,3}$-$2_{0,2}$ and $5_{0,5}$-$4_{0,4}$ transitions that share a rotational level with the drive transition. It is not until 1500 ns pulse duration that transitions that involve levels not directly connected to $4_{0,4}$-$3_{0,3}$ appear in the spectrum. It is noteworthy that these levels differ from the original by $\Delta K_a = 2$ because benzonitrile has C_{2v} symmetry, with nuclear spin symmetries that differ for K_a even and K_a odd (much as in *para*- and *ortho*-H_2O). While such $\Delta K_a = 2$ transitions are not strictly forbidden, their TDMs are factors of 5–15 smaller than their $\Delta K_a = 0$ counterparts (see Table S3) and are not observed in the broadband spectrum. This illustrates the selective nature of the coherence propagation through the rotational manifold.

4-Pentynenitrile has two conformational isomers differing in the dihedral angle about the central C−C single bond, either *trans* (180°) or *gauche* (60°). Further characterization of the broadband microwave spectrum of both conformers of 4-pentyne nitrile will be discussed in a future paper. These conformers are predicted to be separated in energy by 303 cm^{-1}, and both are observed in the supersonic expansion. *Trans* 4-pentynenitrile is the lowest energy conformer; thus, its transitions are significantly more intense than those that belong to the *gauche* conformer.

The *trans* conformer has its main dipole moment along the *a*-axis (3.5 D); therefore, we chose an *a*-type transition ($5_{0,5}$-$4_{0,4}$, 14 480.25 MHz) as resonance step for the SFP experiments. Figure 5(b) shows a series of SFP spectra obtained with microwave power ranging from 10% to 100% of the maximum TWTA output, using a 1 μs pulse duration. Notably, this conformer responds to strong-field SFP excitation much as does E-PVN, where some of the off-resonant transitions do not share either a lower or upper level with the drive transition. Once again, this is puzzling since μ_b is only 0.9 D. The analogous experiment on the *gauche* conformer is shown in Fig. 5(c). This conformer has $\mu_a = 2.2$ D and $\mu_b = 3.4$ D, and in this case, we report results using as resonant excitation $3_{0,3}$-$2_{0,2}$ (12 762.80 MHz). In this case, the SFP experiment shows seven additional transitions of both *a*- and *b*-types that appear and grow in with increasing power.

Finally, the SFP phenomenon was also tested in guaiacol (*o*-methoxy phenol), one of the three aromatic constituents of lignin.[41] This is an interesting molecule to test with SFP excitation because the components of its dipole moment are significantly smaller than the nitriles previously studied ($\mu_a = 2.05$ and $\mu_b = -1.77$). Furthermore, its chemical make-up and sample handling is considerably

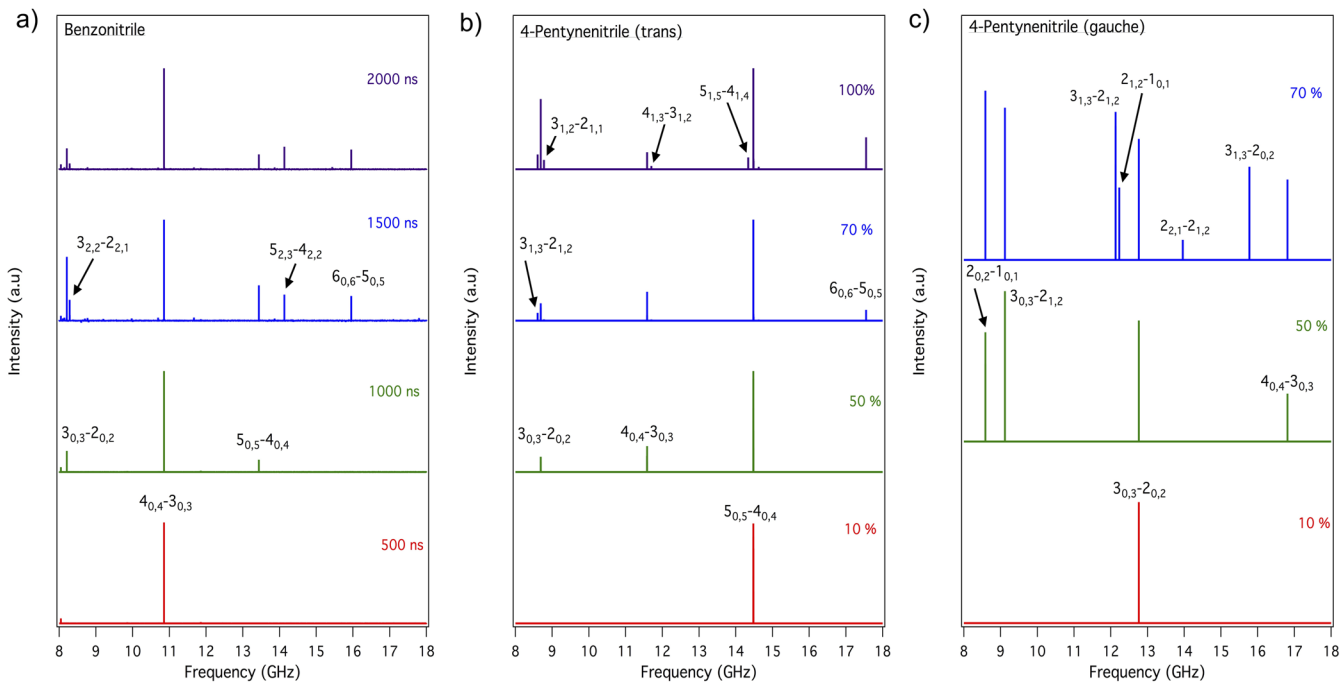

FIG. 5. (a) Single frequency pulse spectra of benzonitrile taken as a function of the time duration of the single-frequency pulse. (b) and (c): Single frequency pulse spectra (1 μs) as a function of percentage of the full microwave power in the TWTA for the *trans* (b) and *gauche* (c) conformers of 4-pentynenitrile. Full-power data on *gauche* 4-pentynenitrile show small signals due to interference from an intense transition of the *trans* conformer ~15 MHz shifted from the transition being modulated, and therefore these data were not included.

different from the nitriles presented to this point. Finally, using a new set of horn antennae that cover the 2–18 GHz range and a new 13 W solid state amplifier (Mercury Systems L0208-41-T113) that covers the 2–8 GHz frequency region, we were able to excite and/or observe signals that covered the entire region from 2 to 18 GHz.

As shown in Fig. 6(a), when using a 1.5 μs SFP resonant with the $3_{0,3}$-$2_{0,2}$ transition of guaiacol, six additional transitions appeared with measurable intensity, even despite the significantly lower power output of the solid-state amplifier. The spectrum in Fig. 6(a) is a composite of two spectra recorded in the 2–8 and the 8–18 GHz regions separately. Furthermore, the fact that these phenomena are robust to the use of a solid-state amplifier and frequency doubler makes it unlikely that nonlinearities in the amplifier could play a role in the off-resonant excitations. Harmonics are present in the TWTA output at full power, as shown in Fig. S4, but at levels less than 10% the main peak. None of the off-resonant transitions appearing in the SFP spectrum are near resonance with these harmonics, nor do other transitions much closer to the harmonics appear.

Figure 6(b) shows the spectrum obtained using a 1 μs SFP resonant with the *b*-type transition $3_{3,0}$-$2_{2,1}$ (14 444.99 MHz). With the TWTA operating at full power (100%), we first recorded in the 8–18 GHz region, observing coherent signals for only two more rotational transitions of guaiacol. Then, with the same TWTA settings, we recorded in the 2–8 GHz region and observed two additional transitions [Fig. 6(b)], the lowest frequency of which ($3_{1,2}$-$2_{2,1}$, 5221.25 MHz) was more than 9 GHz away from the resonant frequency used in SFP excitation.

On the basis of these tests, we conclude that the propagation of molecular coherences under strong-field single-frequency pulse excitation conditions is a quite general molecular phenomenon, exhibiting similar behavior for a range of chemical functionality, maintaining its selectivity in the presence of intermingled transitions from other conformers, following the rules of nuclear spin selectivity and propagating to transitions over a wide frequency range.

E. Collisions

The SFP spectra in Fig. 5(a) for benzonitrile raise a puzzling aspect of the strong-field SFP spectra, namely, that the propagation of molecular coherences through the rotational manifold at times

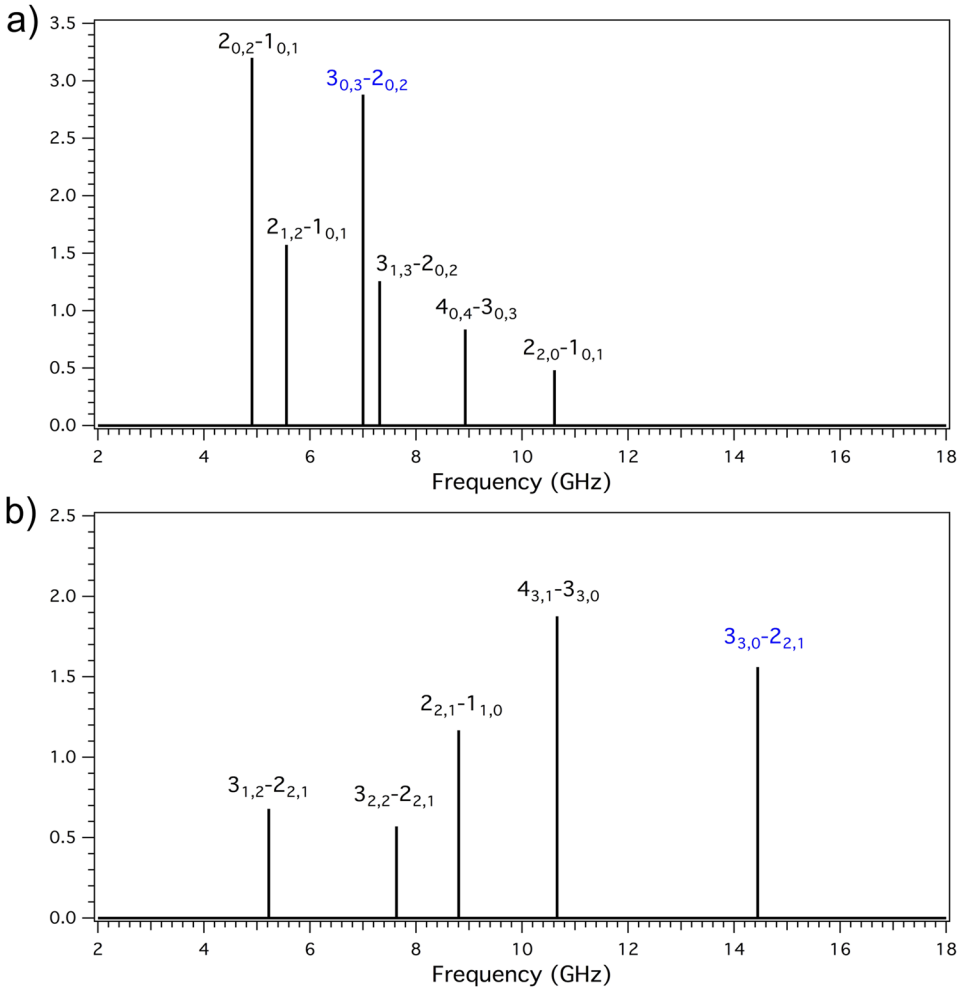

FIG. 6. SFP experiment in guaiacol, with pumped transitions indicated in blue. (a) Single frequency pulse (1.5 μs duration) resonant with the $3_{0,3}$-$2_{0,2}$ transition of guaiacol, taken with a 13 W solid state amplifier. (b) Single frequency pulse (1 μs duration) resonant with the $3_{3,0}$-$2_{2,1}$ transition of guaiacol, taken at 100% TWTA gain.

makes "jumps" to rotational levels that cannot easily be accessed by dipole-allowed transitions. In benzonitrile, this involves transitions out of $K_a = 2$ following resonant excitation of $K_a = 0$-0 transition. This suggests a hypothesis for the appearance of the nonresonant transitions involving collisions with the buffer gas or between the probed molecules could induce coherence transfer in nearby rotational levels. At first glance, this is an odd hypothesis since collisions are typically thought of as destroying coherence rather than transferring it. Nonetheless, the role played by collisions is important to establish. In order to do so, a series of tests was performed, including changing the backing pressure, the carrier gas, the temperature of the sample holder, and the timing of FID collection in the gas pulse.

These tests were also carried out using PVN as the test molecule and with the TWTA set to full power (200 W). The $2_{1,1}$-$1_{1,0}$ (10 052.50 MHz) transition of Z-PVN was used to probe whether changing the backing pressure would change either the intensity or number of off-resonant transitions that appear following SFP excitation. Using He as carrier gas, the backing pressure was increased from 0.30 to 2.40 bars in intervals of 0.70 bar.

As Fig. 7 shows, no significant change was observed as the backing pressure was increased over this range. Indeed, the same 13 transitions appeared in the SFP spectrum in each case, with relative intensities that changed by no more than 5%. We also observed no change in the number of transitions appearing in the SFP spectrum when the helium carrier gas was replaced by neon (Fig. S5).

As the molecules exit the nozzle and undergo a supersonic free jet expansion, they experience many collisions with the buffer gas;

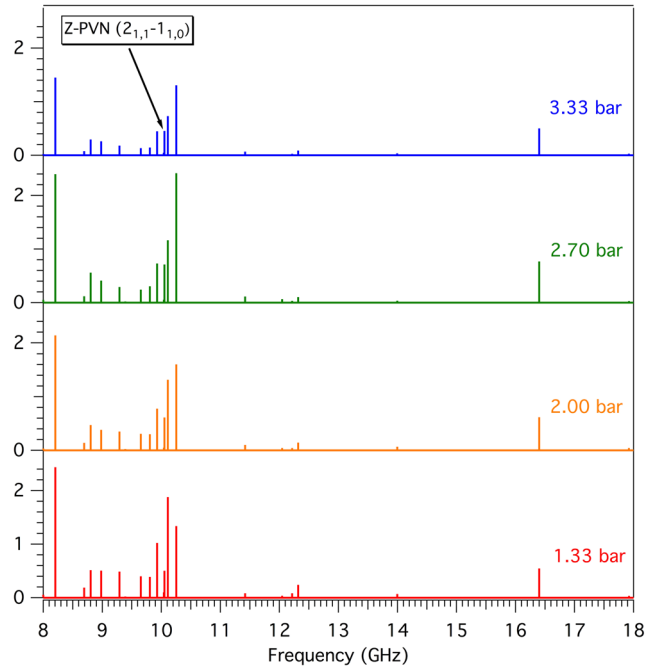

FIG. 7. Comparison of single frequency pulse spectra taken with helium backing pressure behind the pulsed valve of (a)–(d): 1.3, 2.0, 2.7, and 3.4 bars, respectively.

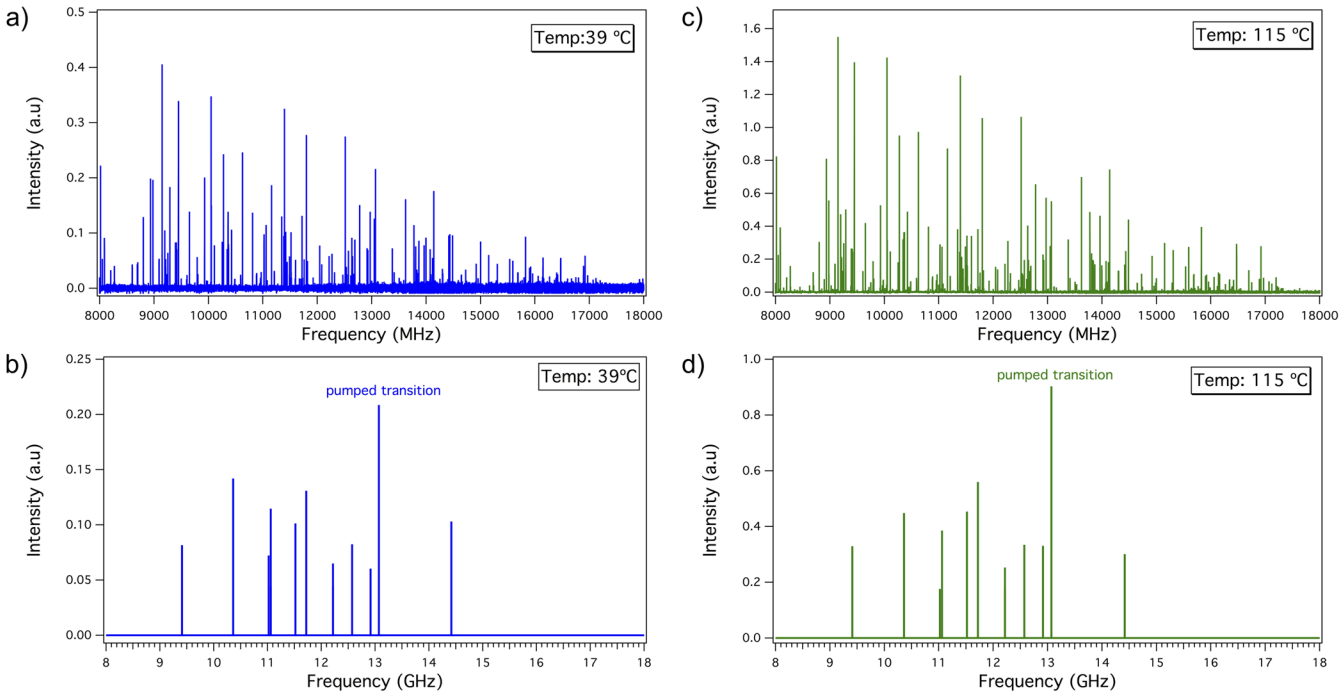

FIG. 8. Broadband microwave [(a) and (c)] and single frequency pulse [(b) and (d)] spectra of PVN taken at two different sample holder temperatures. The blue spectra were taken at 39 °C (VP = 0.057 Torr and 0.005% concentration) and the green spectra were taken at 115 °C (VP = 2.52 Torr and 0.2% concentration) in helium.

nonetheless, as the adiabatic expansion progresses, the expanding gas becomes so rarefied that it is possible to achieve a collision-free environment on the time scale of the molecular FID collection. To test whether having multiple excitations per gas pulse could be having an effect, we recorded an SFP spectrum using a single excitation/FID collection per gas pulse, taken at the optimal delay Δt between opening the pulsed valve and interrogating the gas. Using a 1 μs microwave excitation pulse resonant with the $2_{1,1}$-$1_{1,0}$ Z-PVN transition, the same 13 transitions appeared in the SFP spectrum, confirming that residual coherences were not playing a role in producing the off-resonant transitions.

The previous experiments point to the conclusion that collisions between the carrier gas and the interrogated molecules do not play a major role in the observed phenomena. Even though the molecules responsible for the microwave signal (PVN in this case) are entrained in the carrier gas at a low concentration, we also checked whether PVN-PVN collisions might contribute to the appearance of off-resonant transitions in the SFP experiments. To that end, the $9_{0,9}$-$8_{0,8}$ rotational transition of Z-PVN was probed with a 1 μs single frequency pulse at two different temperatures (39 °C and 115 °C), with the PVN sample entrained in 2.4 bars of He. Figure 8 shows that although the absolute intensity of the transitions grew by a factor of four (i.e., 400%) with the increase in sample temperature, the number and pattern of the modulated transitions was virtually unchanged, with changes relative to the resonant transition of less than 20%.

Using the room temperature equilibrium vapor pressure for PVN and the Clausius-Clapeyron equation (with ΔH_{vap} = 50.2 kJ/mol), PVN's equilibrium vapor pressure and percent concentration in the expansion at 39 °C are ~0.057 Torr and 2.5 × 10^{-3}%, respectively. At 115 °C, the vapor pressure and equilibrium concentration are nearly 40 times larger (2.52 Torr, 0.1%). The fact that the signal change was only a factor of four instead of 40 indicates that at the helium flows being used (1.4 bars $cm^3 \cdot s^{-1}$), the full equilibrium vapor pressure of PVN is not reached. Nevertheless, on the basis of this test and the previous backing pressure studies, it seems unlikely that molecule-carrier gas or molecule-molecule collisions could play a significant role in contributing to the presence and intensity of off-resonant molecular transitions in the strong-field SFP experiments.

V. DISCUSSION

Armed with this set of experimental observations, simulations were carried out using the time-dependent quantum model(s) described in Sec. III. The calculations reproduce many of the nonresonant frequencies that are observed experimentally when the microwave pulses that are used have window functions in which the turn-on or turn-off occurs over a period of less than 20 cycles. However, for the calculation, almost all of the nonresonant frequencies disappear for longer turn on/off times, including the shortest turn on/off times achieved experimentally, equivalent to about 50 frequency cycles. The fact that many of the frequencies that are seen in the experiment are also in the unphysically short turn-on/off calculations might mean that the molecules behave like the microwaves are only present for a short time duration; however, this observation is ruled out by experimental data [Fig. 4(a)]. The modeled results are consistent with the fact that the presence or absence of the nondriven frequencies was not affected by the duration of the SFP once the number of Rabi oscillations was larger than a few.

One of the written programs included a full density matrix, where an N × N matrix was propagated (N being the number of states), allowing the molecule to start in all of the states with the appropriate Maxwell-Boltzmann weight. This program was compared with calculations that use single states, and the results were the same when including the same states (as it should when decoherence is not present). However, none of the programs were able to reproduce the increase in number of transitions, with respect to power level and pulse duration, that is observed in the experiment. In all calculations, the range of states was increased until the calculated FID was converged. We were able to converge all of the calculations although the computational effort increases rapidly with the range of states included.

A completely different approach was to take the states involved in the experimental off-resonant modulated transitions and solve the density matrix equation only for those states. For example, for the $9_{0,9}$-$8_{0,8}$ (13 069.37 MHz) transition of Z-PVN, the energies and dipoles of the states $7_{0,7}$, $7_{1,7}$, $8_{0,8}$, $8_{1,8}$, $9_{0,9}$, $9_{1,9}$, $10_{0,10}$, and $10_{1,10}$ were used. This is a much faster program that gave results similar to the full calculation and was used to quickly test ideas.

While our experimental tests indicate that collisions are not playing a defining role, we thought it is still important to think through the possibility that rotational coherence transfer might occur during a soft collision from one J_{KaKc} level to another that is nearby in energy, without losing the phase information. To get some sense for the types of collisions that might occur, we estimated collision rates in one of two ways. First, we assumed hard-sphere collisions between He and PVN to occur at the known rotational temperature of the expansion, T_{rot} ~ 1 K, which produces a time between collisions of 28 μs at 10 cm from the valve orifice. This is the normal circumstance of collisional dephasing. By comparison, we estimated the distance of closest approach needed for a dipole-induced dipole interaction of He with a PVN molecule to have an interaction energy that is stronger than the ΔE associated with a ΔK_a = 1 changing collision (for example). Under these conditions, the collision cross sections are about ten times larger than hard sphere, with the He atom having a maximum impact parameter of 12 Å from the PVN center-of-mass, resulting in a "fly by" collision occurring in about 20 ps. The time between such collisions is about 2.8 μs, and there are about 30–40 such collisions during the traversal of PVN through the horns. By comparison, the T_1 decay time of the experimental molecular FID is about 3 μs, indicating that these gentle collisions could be leading to decoherence.

We added mechanisms that mimic collisions into the simulations that use wavefunctions averaged over random collision times or density matrix treatments. As expected, both treatments led to smaller FID signals for the resonance transitions with no indication of sidebands. We also tested whether the dipole-dipole interactions between pairs of molecules are important (Förster resonant exchange[42]) by making a wave function program that simultaneously solved for the effect of microwaves on two molecules that included their coupling with each other through the dipole-dipole interaction. Again, the effect was too small to account for observation.

Besides collisions, we tested several possible mechanisms as the source for the extra transitions. The simplest mechanism tested was to make the microwave fields up to twice as strong as the upper limits of the experimental estimates. Another possible mechanism tested was whether the collective polarization of the gas could lead to a non-negligible change in electric field due to the average dielectric properties of the gas. This possibility was ruled out because the estimated change in electric field due to the susceptibility was much too small to account for the effects. A third mechanism considered was the possibility for super-radiant spontaneous emission[43] that arises because there is an inversion in the rotational population under conditions where many are within a wavelength of each other. At its largest, this decay rate is the surplus of molecules in the excited state of a pair of dipole-connected states times the spontaneous decay rate.[44] Although the surplus could be large, the spontaneous decay rate of a single molecule is tiny due to the small energy difference of these states, and thus this effect also could not account for the observed magnitude of the off-resonant transitions.

VI. CONCLUSIONS

A new phenomenon has been observed when high-powered, monochromatic microwave pulses interact with jet-cooled molecular rotational levels under conditions in which the resonant microwave transition is driven through many Rabi cycles. Coherences are observed in off-resonant rotational transitions at sufficient intensity to be easily detected. These off-resonant transitions are only in the species resonantly excited. A series of tests using E- and Z-phenylvinylnitrile were conducted to assess the conditions required to produce observable signals in off-resonant transitions. As the power of the electric field or the duration of the pulse increases, the number of off-resonant transitions increases, beginning with rotational transitions that share lower or upper levels with the driven transitions, but propagating out into a wider manifold of levels at higher powers/longer pulse durations. Therefore, it was surmised that the number of Rabi cycles was crucial to the appearance of off-resonant transitions in the molecular signal. To make sure that these effects were not unique to a particular molecule, similar SFP experiments were carried out on benzonitrile, 4-pentynenitrile, and guaiacol. In each case, the same qualitative behavior was observed. The effects of collisions were tested by changing the backing pressure of the carrier gas, the concentration of PVN in the gas mixture, and by testing different sections of the gas pulse. All our tests pointed to collisions not contributing in a significant way to the off-resonance transitions.

A time-dependent quantum model for the interaction of the microwave field with the ensemble of rotating molecules has been developed to compare with the experimental results. The standard time-dependent quantum model implemented here does not account for the novel features present in the experimental results, most notably in not predicting the intensity and growing number of off-resonant transitions with increasing pulse power and/or duration. It is clear that the model is missing a key factor, yet to be determined.

Nonetheless, this experimental discovery, in which a single frequency pulse in the strong field regime produces measurable coherent signals from other species-specific transitions, is likely to speed the analysis of microwave spectra since the off-resonant transitions not only help deconvolute the spectrum but also establish the connectivity of the transitions, which grow and spread with increasing power/pulse duration from the two levels initially involved in the resonant transition. In addition, as the physical mechanism is clarified, the possibility of using such strong-field phenomena to create and control molecular coherences offers interesting prospects for quantum entanglement and quantum sensors.

SUPPLEMENTARY MATERIAL

See supplementary material for (i) a description of the Matlab program that calculated the transition matrix elements, (ii) a description of some of the window functions that were used, (iii) details of the collision calculations, (iv) SFP spectra of E-PVN, (v) the molecular rotational parameters for E– and Z-PVN, and (vi) a comparison of SFP spectra of Z-PVN recorded using different carrier gases.

ACKNOWLEDGMENTS

C.A. and T.S.Z. gratefully acknowledge support for this research from the Department of Energy Basic Energy Sciences, Chemical Sciences Division, under Grant No. DEFG02-96ER14656. A.O.H.-C. and T.S.Z. also acknowledge the Donors of the American Chemical Society Petroleum Research Fund for partial support for this research through a New Directions Grant No. PRF #55152-ND6. F.R. was supported by the Department of Energy, Office of Science, Basic Energy Sciences, under Award No. DE-SC0012193.

REFERENCES

[1] J.-U. Grabow, in *Handbook of High-Resolution Spectroscpy*, edited by M. Quack and F. Merkt (Wiley, 2011), p. 723.
[2] J. C. McGurk, T. G. Schmalz, and W. H. Flygare, J. Chem. Phys. **60**, 4181 (1974).
[3] J. C. McGurk, H. Mäder, R. T. Hofmann, T. G. Schmalz, and W. H. Flygare, J. Chem. Phys. **61**, 3759 (1974).
[4] T. Kasuga, T. Amano, and T. Shimizu, Chem. Phys. Lett. **42**, 278 (1976).
[5] W. E. Hoke, D. R. Bauer, and W. H. Flygare, J. Chem. Phys. **67**, 3454 (1977).
[6] B. Vogelsanger, A. Bauder, and H. Mäder, J. Chem. Phys. **91**, 2059 (1989).
[7] J. U. Grabow, Angew. Chem., Int. Ed. Engl. **52**, 11698 (2013).
[8] G. G. Brown, B. C. Dian, K. O. Douglass, S. M. Geyer, S. T. Shipman, and B. H. Pate, Rev. Sci. Instrum. **79**, 053103 (2008).
[9] G. B. Park and R. W. Field, J. Chem. Phys. **144**, 200901 (2016).
[10] T. J. Balle and W. H. Flygare, Rev. Sci. Instrum. **52**, 33 (1981).
[11] T. G. Schmalz and W. H. Flygare, *Coherent Transient Microwave Spectroscopy and Fourier Transform Methods* (Springer, 1978).
[12] D. Schmitz, V. Alvin Shubert, T. Betz, and M. Schnell, J. Mol. Spectrosc. **280**, 77 (2012).
[13] N. V. Vitanov, T. Halfmann, B. W. Shore, and K. Bergmann, Annu. Rev. Phys. Chem. **52**, 763 (2001).
[14] P. Dietiker, E. Miloglyadov, M. Quack, A. Schneider, and G. Seyfang, J. Chem. Phys. **143**, 244305 (2015).
[15] K. Bergmann, N. V. Vitanov, and B. W. Shore, J. Chem. Phys. **142**, 170901 (2015).
[16] C. Abeysekera, A. O. Hernandez-Castillo, J. F. Stanton, and T. S. Zwier, J. Phys. Chem. A **122**, 6879 (2018).
[17] S. M. Fritz, B. M. Hays, A. O. Hernandez-Castillo, C. Abeysekera, and T. S. Zwier, Rev. Sci. Instrum. **89**, 093101 (2018).
[18] K. Prozument, Y. V. Suleimanov, B. Buesser, J. M. Oldham, W. H. Green, A. G. Suits, and R. W. Field, J. Phys. Chem. Lett. **5**, 3641 (2014).

[19]C. Abeysekera, B. Joalland, N. Ariyasingha, L. N. Zack, I. R. Sims, R. W. Field, and A. G. Suits, J. Phys. Chem. Lett. **6**, 1599 (2015).
[20]G. B. Park, C. C. Womack, A. R. Whitehill, J. Jiang, S. Ono, and R. W. Field, J. Chem. Phys. **142**, 144201 (2015).
[21]D. Schmitz, V. A. Shubert, D. Patterson, A. Krin, and M. Schnell, J. Phys. Chem. Lett. **6**, 1493 (2015).
[22]J. L. Neill, S. T. Shipman, L. Alvarez-Valtierra, A. Lesarri, Z. Kisiel, and B. H. Pate, J. Mol. Spectrosc. **269**, 21 (2011).
[23]M. A. Martin-Drumel, M. C. McCarthy, D. Patterson, B. A. McGuire, and K. N. Crabtree, J. Chem. Phys. **144**, 124202 (2016).
[24]D. Patterson and J. M. Doyle, Phys. Rev. Lett. **111**, 023008 (2013).
[25]Y. Zhou, D. D. Grimes, T. J. Barnum, D. Patterson, S. L. Coy, E. Klein, J. S. Muenter, and R. W. Field, Chem. Phys. Lett. **640**, 124 (2015).
[26]A. O. Hernandez-Castillo, C. Abeysekera, B. M. Hays, and T. S. Zwier, J. Phys. Chem. A **145**, 114203 (2016).
[27]P. S. Shternin, K.-H. Gericke, and O. S. Vasyutinskii, Mol. Phys. **108**, 813 (2010).
[28]B. W. Shore and P. L. Knight, J. Mod. Opt. **40**, 1195 (1993).
[29]D. D. Grimes, S. L. Coy, T. J. Barnum, Y. Zhou, S. F. Yelin, and R. W. Field, Phys. Rev. A **95**, 043818 (2017).
[30]D. D. Grimes, T. J. Barnum, Y. Zhou, A. P. Colombo, and R. W. Field, J. Chem. Phys. **147**, 144201 (2017).
[31]J. M. Martinis, S. Nam, J. Aumentado, and C. Urbina, Phys. Rev. Lett. **89**, 117901 (2002).
[32]C. Karunatilaka, A. J. Shirar, G. L. Storck, K. M. Hotopp, E. B. Biddle, R. Crawley, and B. C. Dian, J. Phys. Chem. Lett. **1**, 1547 (2010).
[33]G. B. Park and R. W. Field, J. Mol. Spectrosc. **312**, 54 (2015).
[34]J. S. Briggs and J. M. Rost, Eur. Phys. J. D **10**, 311 (2000).
[35]H. Friedrich, *Theoretical Atomic Physics* (Springer-Verlag, 1990).
[36]J. F. Kaiser and F. F. Kuo, *System Analysis by Digital Computer* (John Wiley & Sons, 1966), pp. 232–235.
[37]J. W. Tukey, *An Introduction to the Calculations of Numerical Spectrum Analysis*, The Spectral Analysis of Time Series, edited by B. Harris (Wiley, New York, 1967), pp. 25–46.
[38]P. Bloomfield, *Fourier Analysis of Time Series: An Introduction* (Wiley-Interscience, New York, NY, 2000).
[39]C. J. Foot, *Atomic Physics* (OU Press, Great Britain, 2005).
[40]H. M. Pickett, J. Mol. Spectrosc. **148**, 371 (1991).
[41]J. Huang, X. Li, D. Wu, H. Tong, and W. Li, J. Renewable Sustainable Energy **5**, 043112 (2013).
[42]S. Ravets, H. Labuhn, D. Barredo, L. Béguin, T. Lahaye, and A. Browaeys, Nat. Phys. **10**, 914 (2014).
[43]R. G. DeVoe and R. G. Brewer, Phys. Rev. Lett. **76**, 2049 (1996).
[44]R. H. Dicke, Phys. Rev. **93**, 99 (1954).